Citation:
Bui, L, Pelusi, M, Vo, T, Sarkhosh, N, Emami, H, Eggleton, B and Mitchell, A 2009, 'Instantaneous frequency measurement system using optical mixing in highly nonlinear fiber', Optics Express, vol. 17, no. 25, pp. 22983-22991.

Instantaneous frequency measurement system using optical mixing in highly nonlinear fiber

Lam A. Bui,[1,*] Mark D. Pelusi,[2] Trung D. Vo,[2] Niusha Sarkhosh,[1] Hossein Emami,[1] Benjamin J. Eggleton,[2] and Arnan Mitchell[1]

[1]*School of Electrical and Computer Engineering, ARC Centre for Ultra-high bandwidth Devices for Optical Systems, RMIT University, Melbourne, VIC 3001, Australia*
[2]*School of Physics, Institute of Photonics and Optical Science, ARC Centre for Ultrahigh-bandwidth Devices for Optical Systems, University of Sydney, NSW 2006, Australia*
**lam.bui@rmit.edu.au*

Abstract: A broadband photonic instantaneous frequency measurement system utilizing four-wave mixing in highly nonlinear fiber is demonstrated. This new approach is highly stable and does not require any high-speed electronics or photodetectors. A first principles model accurately predicts the system response. Frequency measurement responses from 1 to 40 GHz are demonstrated and simple reconfiguration allows the system to operate over multiple bands.

OCIS codes: (0060.5625) Radio frequency photonics; (060.2360) Fiber optics links and subsystems; (350.4010) Microwaves; (190.4223) Nonlinear wave mixing.

References and links

1. J. Capmany, and D. Novak, "Microwave photonics combines two worlds," Nat. Photonics **1**(6), 319–330 (2007).
2. A. J. Seeds, "Microwave photonics," IEEE Trans. Microw. Theory Tech. **50**(3), 877–887 (2002).
3. R. Helkey, J. V. Twinchel, and C. Cox, "A down-conversion optical link with RF gain," J. Lightwave Technol. **15**(6), 956–961 (1997).
4. R. A. Minasian, "Photonic signal processing of microwave signals," IEEE Trans. Microw. Theory Tech. **54**(2), 832–846 (2006).
5. A. Lindsay, G. Knight, and S. Winfall, "Photonic Mixers for wide bandwidth RF receiver Applications," IEEE Trans. Microw. Theory Tech. **43**(9), 2311–2317 (1995).
6. R. D. Esman, M. Y. Frankel, J. L. Dexter, L. Goldberg, M. G. Parent, D. Stilwell, and D. G. Cooper, "Fiber-optic prism true time-delay antenna feed," IEEE Photon. Technol. Lett. **5**(11), 1347–1349 (1993).
7. H. Emami, N. Sarkhosh, L. A. Bui, and A. Mitchell, "Wideband RF photonic in-phase and quadrature-phase generation," Opt. Lett. **33**(2), 98–100 (2008).
8. L. V. T. Nguyen, and D. B. Hunter, "A Photonic technique for microwave frequency measurement," IEEE Photon. Technol. Lett. **18**(10), 1188–1190 (2006).
9. N. Sarkhosh, H. Emami, L. Bui, and A. Mitchell, "Reduced cost photonic instantaneous frequency measurement system," IEEE Photon. Technol. Lett. **20**(18), 1521–1523 (2008).
10. G. P. Agrawal, Nonlinear Fiber Optics (Academic Press, San Diego, 2001).
11. S. Radic, D. J. Moss, and B. J. Eggleton, "Nonlinear Optics in Communications: From Crippling Impairment to Ultrafast Tools" in Optical Fiber Telecommunications V: Components and Sub-systems, I. P. Kaminow, T. Li, and A. E. Willner, ed. (Academic Press, Oxford, UK, February 2008), Chap. 20.
12. J. Li, B. E. Olsson, and M. Karlsson, and P. A. Andrekson, "OTDM demultiplexer based on XPM-induced wavelength shifting in highly nonlinear fiber," IEEE Photon. Technol. Lett. **15**(12), 1770–1772 (2003).
13. V. G. Ta'eed, M. Shokooh-Saremi, L. Fu, I. C. M. Littler, D. J. Moss, M. Rochette, B. J. Eggleton, B. Yinlan Ruan, and B. Luther-Davies, "Self-phase modulation-based integrated optical regeneration in chalcogenide waveguides," IEEE J. Sel. Top. Quantum Electron. **12**(3), 360–370 (2006).
14. J. Capmany, S. Sales, D. Pastor, and B. Ortega, "Optical mixing of microwave signals in a nonlinear semiconductor laser amplifier modulator," Opt. Express **10**(3), 183–189 (2002).
15. M. Pelusi, F. Luan, T. D. Vo, M. R. E. Lamont, S. J. Madden, D. A. Bulla, D.-Y. Choi, B. Luther-Davies, and B. J. Eggleton, "Photonic-chip-based radio-frequency spectrum analyser with terahertz bandwidth," Nat. Photonics **3**(3), 139–143 (2009).
16. H. Cuckson, and P. D. Curtis, "Microwave instantaneous frequency measurement apparatus," United States Patent 4414505, 8 Nov. (1983).
17. G.-C. Liang, C.-F. Shih, R. S. Withers, B. F. Cole, M. E. Johansson, and L. P. Suppan, Jr., "Superconductive digital instantaneous frequency measurement subsystem," IEEE Trans. Microw. Theory Tech. **41**(12), 2368–2375 (1993).

#114537 - $15.00 USD Received 20 Jul 2009; revised 8 Oct 2009; accepted 12 Nov 2009; published 1 Dec 2009

18. U. Gliese, S. Norskov, and T. N. Nielsen, "Chromatic dispersion in fiber-optic microwave and millimeter-wavelinks," IEEE Trans. Microw. Theory Tech. **44**(10), 1716–1724 (1996).
19. N. Sarkhosh, H. Emami, L. Bui, and A. Mitchell, "Microwave photonic instantaneous frequency measurement with improved sensitivity," In *Proceedings of IEEE International Microwave Symposium (IMS 2009)*, 165–168. (2009)
20. H. Emami, N. Sarkhosh, L. A. Bui, and A. Mitchell, "Amplitude independent RF instantaneous frequency measurement system using photonic Hilbert transform," Opt. Express **16**(18), 13707–13712 (2008).

1. Introduction

Microwave photonics (MWP) has become an established technology for analogue distribution of high-frequency signals with applications in both wireless communications and radar systems [1,2]. In such systems, lightweight, moderate span (1km) optic fibers separate simple passive antennas from sensitive, expensive and bulky electronic signal processing units [3]. These photonically remoted systems offer the opportunity for optical processing of the analogue RF signal prior to electronic detection [4]. Some prominent examples of MWP signal processing systems include mixing [5], filtering [4], time-delay [6], phase transformation [7] and optical frequency measurement [8,9]. In each of these systems functionality is achieved using passive optics or RF driven optical modulation.

Recently, nonlinear optics has emerged as a powerful tool for ultra-fast optical signal processing [10,11]. Interest has been driven by the potential for ultra-fast manipulation of digital signals [12,13], but recently research effort has extended to the use of nonlinear optics for MWP signal processing. Nonlinear mechanisms that have been studied for MWP applications include cross-gain modulation in semiconductor devices [14] and cross phase modulation and four-wave mixing in optical fibers and integrated optic waveguides [15]. Nonlinear optics offers the key advantage of performing high-speed signal processing in the optical domain, such that multi-octave bandwidth receiving electronics are no longer required.

In this paper we present the first demonstration of an instantaneous frequency measurement system [16] using four-wave mixing within Highly Non-Linear Fiber (HNLF). This implementation offers the specific advantage of measuring a broad frequency range of RF input frequencies but without the requirement for high speed electronic components at any stage of the system, and in particular requiring only DC photo-detectors at the output. This feature reduces overall system cost and greatly simplifies associated receiving electronics, especially when multiple parallel systems are required. The system is stable and highly predictable enabling accurate mapping of the output optical power to the input RF frequency. The system frequency band can be readily reconfigured and could be extended to perform several parallel frequency measurements with only a modest increase in component count.

2. Principle of operation

An instantaneous frequency measurement (IFM) system is a low latency tool that is often used in radar systems for detecting and roughly classifying unknown signals [16]. Figure 1(a) and 1(b) present two examples of IFM systems [16,17]. The frequency response is a sinusoid with period $1/\Delta t$. If Δt is known, a measurement of the output level can be used to infer the input RF frequency. The approach of Fig. 1(a) has the advantage of simple implementation, but expensive detection hardware may be required to measure the broadband RF output power. The approach of Fig. 1(b) has a DC output, which simplifies the receiver electronics, but relies on broadband mixing, which can be challenging with traditional RF techniques. An optimal compromise between both approaches may be possible with photonics.

#114537 - $15.00 USD Received 20 Jul 2009; revised 8 Oct 2009; accepted 12 Nov 2009; published 1 Dec 2009

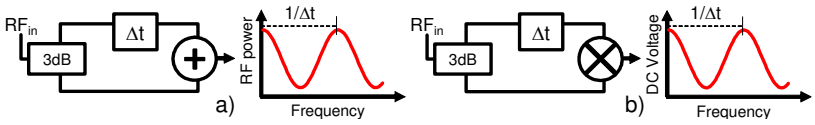

Fig. 1. IFM approaches: a) RF power summation technique [16] and b) Phase discrimination technique [17].

3. Four-wave mixing based instantaneous frequency measurement

The principle of our FWM based IFM scheme is summarized in Fig. 2. The key feature of this approach is that the frequency measurement is obtained as the DC optical power at an inexpensive, low frequency detector. Our approach can be explained theoretically as follows.

Consider two optical carriers (at frequencies ω_1 and ω_2). Carrier ω_1 is modulated by the RF signal to be measured (at frequency Ω). This input field can be written as:

$$E = Ae^{j\omega_1 t} + Be^{j((\omega_1+\Omega)t+\varphi_1)} + Be^{j((\omega_1-\Omega)t+\varphi_2)} + Ae^{j\omega_2 t} + CC \qquad (1)$$

where A and B are the amplitudes of the carrier and RF sidebands respectively and CC denotes complex conjugate. The terms ϕ_1 and ϕ_2 are phase differences between the carrier and sidebands which can accumulate due to dispersion and are functions of RF frequency [18].

Typical nonlinear systems exhibit third order behavior leading to effects such as self phase modulation and four-wave mixing (FWM) [10]. FWM is a parametric process that is often observed as a strong pump transferring power to a carrier and producing an idler. In Eq. (1) there are two pumps of amplitude (A) and two signals of amplitude (B) and thus the mixing products are more complex than the traditional signal/ idler/ pump configuration often reported [10]. However, it is well known that the harmonic products created by the third order nonlinearity will be proportional to the cube of the electric field. Thus taking the cube of Eq. (1) and assuming $A>>B$, and retaining only terms close to ω_1 and ω_2 we find:

$$\begin{aligned} E^3 = \{ & \; 3Ae^{j\omega_1 t} + 4Be^{j((\omega_1+\Omega)t+\varphi_1)} + Be^{j((\omega_1+\Omega)t-\varphi_2)} + 4Be^{j((\omega_1-\Omega)t+\varphi_2)} + Be^{j((\omega_1-\Omega)t-\varphi_1)} \\ & + 3Ae^{j\omega_2 t} + 2Be^{j((\omega_2+\Omega)t+\varphi_1)} + 2Be^{j((\omega_2+\Omega)t-\varphi_2)} + 2Be^{j((\omega_2-\Omega)t+\varphi_2)} + 2Be^{j((\omega_2-\Omega)t-\varphi_1)} \\ & + Ae^{j(\omega_1-\Delta\omega)t} + 2Be^{j((\omega_1-\Delta\omega+\Omega)t+\varphi_1)} + 2Be^{j((\omega_1-\Delta\omega-\Omega)t+\varphi_2)} \\ & + Ae^{j(\omega_2+\Delta\omega)t} + Be^{j((\omega_2+\Delta\omega+\Omega)t-\varphi_2)} + Be^{j((\omega_2+\Delta\omega-\Omega)t-\varphi_1)} \; \} 3A^2 + CC \end{aligned} \qquad (2)$$

where $\Delta\omega = \omega_2-\omega_1$. The carrier at ω_2 now has RF sidebands and new idler channels appear at ($\omega_1-\Delta\omega$ and $\omega_3 + \Delta\omega$) as expected. The change of sign on some of the dispersion terms (ϕ_1 and ϕ_2) highlight the fact that phase conjugation occurs during FWM [10]. In calculating Eq. (2) it has been assumed that the dispersion within the HNLF is insignificant.

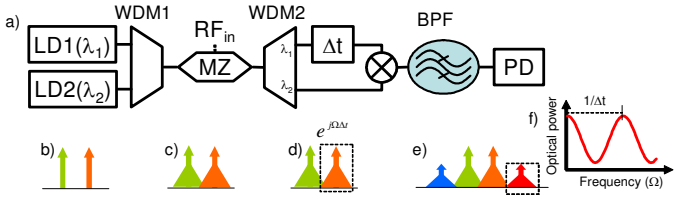

Fig. 2. Principle of Photonic IFM system using FWM: a) Illustrative schematic system b) optical carriers of equal power at two different wavelengths; c) carriers combined and modulated with the same RF signal; d) carriers separated and differentially delayed by time Δt; e) carriers mixed are mixed using nonlinear element producing idlers which coherently combine signals from both carriers; power at idler is separated with filter and measured by DC photo-detector; f) output power oscillates with frequency providing IFM function.

#114537 - $15.00 USD Received 20 Jul 2009; revised 8 Oct 2009; accepted 12 Nov 2009; published 1 Dec 2009

To achieve the IFM function of Fig. 2, we must combine two differentially delayed versions of the same signal. Thus, if we now also modulate the carrier at ω_2 with the same signal at RF frequency Ω, but delay this carrier by Δt, then the input field can be written:

$$E = Ae^{j\omega_1 t} + Be^{j((\omega_1+\Omega)t+\varphi_1)} + Be^{j((\omega_1-\Omega)t+\varphi_2)} + Ae^{j\omega_2(t+\Delta t)} + Be^{j((\omega_2+\Omega)(t+\Delta t)+\varphi_3)} + Be^{j((\omega_2-\Omega)(t+\Delta t)+\varphi_4)} + CC \quad (3)$$

Again if we take the cube of Eq. (3) and assume $B<<A$, and consider only the idler at $(\omega_1-\Delta\omega)$ and its sidebands, we find:

$$E^3 = 3A^2 e^{j(\omega_1-\Delta\omega)t} e^{-j\omega_2\Delta t}\left\{A + 2Be^{j(\Omega t+\varphi_1)} + 2Be^{-j(\Omega t-\varphi_2)} + Be^{j(\Omega t+\Omega\Delta t-\varphi_4)} + Be^{-j(\Omega t+\Omega\Delta t+\varphi_3)} + CC\right\} \quad (4)$$

Comparing Eq. (4) to Eq. (2) it appears that the sidebands now include the summation of the RF signals mixed from channel ω_1 and channel ω_2. This summation is coherent and hence the optical power itself varies. Thus this nonlinear photonic approach actually implements the summation concept of Fig. 1(a). If we measure only the lower idler, we find:

$$P(\omega_1-\Delta\omega) \propto \{A^2 + B^2[5+4\cos(\Omega\Delta t-\varphi_1-\varphi_4)] + B^2[5+4\cos(\Omega\Delta t+\varphi_2+\varphi_3)]\} \quad (5)$$

Eq. (5) shows that the idler power oscillates with RF frequency (Ω), and thus, if the time delay (Δt) and the dispersion characteristics (ϕ_1,ϕ_2,ϕ_3 and ϕ_4) are known, the frequency can be inferred from the this idler power. The proposed configuration is actually a summation system (see Fig. 1(a)), but offers a DC power output similar to a phase correlation system (see Fig. 1(b)).

Before proceeding with demonstration of our proposed HNLF based IFM we must characterize a practical HNLF to insure that it does indeed behave according to these simple predictions and that it maintains this behavior over the whole RF band from 1 to 40 GHz.

4. Characterization of analogue all-optical mixing using highly nonlinear fiber

Figure 3 presents the configuration used to characterize microwave photonic all optical mixing. Two lasers (LD1 and LD2) generated optical carriers at λ_1 and λ_2. An RF tone was modulated onto carrier λ_1 via a broadband Mach-Zehnder modulator (MZ). The two carriers were combined using a 3 dB coupler and launched into a Cascaded Fiber Bragg Grating (CFBG) which reflected different wavelengths from different locations along the fiber length imparting a relative time delay. The combined carriers were amplified using an Erbium Doped Fiber Amplifier (EDFA) and then launched into the HNLF (1km of OFS Standard HNLF - zero dispersion at 1540 nm, dispersion slope: 0.019 ps/(nm^{2}km), gamma: 21/W/km). All system components up to the HNLF were polarization maintaining. At the HNLF output, a small amount of power was monitored using an Optical Spectrum Analyzer (OSA, resolution 0.05nm). The idler at λ_1-$\Delta\lambda$ (where $\Delta\lambda = \lambda_2-\lambda_1$) was isolated using an arrayed waveguide grating (AWG, ANDevices DWDM-F-100G) and the power was measured using a 50 GHz photo-detector (u^{2}t XPDV2020R) connected to an Electrical Spectrum Analyzer (ESA).

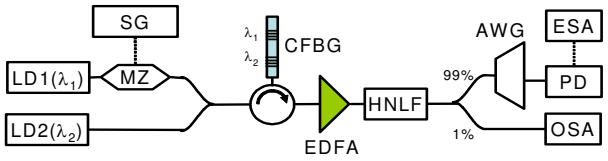

Fig. 3. HNLF characterization system: Lasers (LD1 & LD2) provide carriers (λ_1 & λ_2). Signal generator (SG) provides RF signal to modulate λ_1 via Mach-Zehnder (MZ). λ_1 and λ_2 are combined and λ_2 is delayed by a cascated fibre Bragg grating (CFBG). λ_1 & λ_2 are amplified by an EDFA and mixed using HNLF. The output is monitored by an OSA. An AWG separates the idler at $\lambda_1 - \Delta\lambda$ (where $\Delta\lambda = \lambda_2-\lambda_1$). A broadband photo-detector (PD) and ESA measures the RF signal.

#114537 - $15.00 USD Received 20 Jul 2009; revised 8 Oct 2009; accepted 12 Nov 2009; published 1 Dec 2009

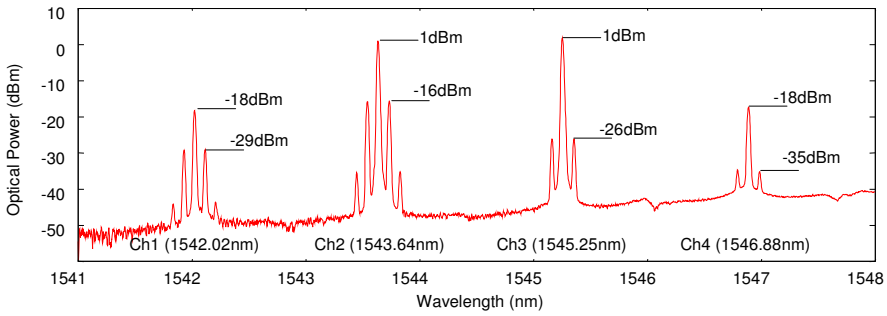

Fig. 4. OSA spectrum of the output of Fig. 2. Ch2 is amplitude modulated with signal at 12 GHz and mixed with un-modulated Ch3 through the HNLF. The powers of various components are indicated.

Using the setup of Fig. 3, LD1 and LD2 were set to λ_1 = 1543.64 nm and λ_2 = 1545.25 nm which were within the zero dispersion wavelength range of the used HNLF. These wavelengths were called Channel 2 and Channel 3 respectively. The modulator was biased at quadrature and the signal generator output was maintained at 10 dBm RF power (modulation depth approx. 20% at 1GHz) throughout the experiment. The lasers were adjusted to provide the same power (~10 dBm) at the HNLF input. The AWG output was monitored for signals at 1542.02 nm (Channel 1).

Figure 4 presents the OSA spectrum recorded at the output of the HNLF when the input RF frequency was set to 12GHz. This spectrum can be compared to the predictions of Eq. (2). The HNLF has mixed the signals on Channel 2 and Channel 3 to create idlers at Channel 1 (1542.02 nm) and Channel 4 (1456.88 nm) via FWM. The mixing efficiency can be seen to be −19 dB. A higher mixing gain may be achieved with stronger optical carriers; however, we have used optical powers that are typical of commodity communications systems.

The modulation of Channel 2 with 10 dBm RF power has resulted in sidebands that are −17 dB down from the carrier. According to Eq. (2), the upper idler on Channel 4 should be a scaled replica of the modulated signal on Channel 2. The carrier on Channel 4 is at −18 dBm and the sidebands are at −35 dBm, so the ratio of −17 dB is maintained. According to Eq. (2), the ratio of carrier and sideband amplitude for the lower idler (Channel 1) should be double the original (Channel 2) and thus the relative power in the sidebands should be 4 times the original. The carrier on Channel 1 is −18 dBm (identical to Channel 4), however the sidebands are −29 dBm. This ratio of sideband to carrier is −11 dB which is 6 dB higher than the −17 dB ratio observed on Channel 2 and Channel 4. It has thus been demonstrated that Eq. (2) does provide an excellent prediction of the practical FWM behavior in practical HNLF.

Channel 3 was not modulated before the HNLF, but has acquired sidebands through nonlinear mixing. This is expected from Eq. (2); however the magnitude of these sidebands is approximately 3 dB lower than predicted. It should be noted that, according to Eq. (2) the sidebands added to Channel 3 are scaled by the vector summation of components with different phases (ϕ_1 and ϕ_2). Significant dispersion can be expected due to reflection from the CFBG in Fig. 3 and the reduction in sideband magnitude observed for Channel 3 in Fig. 4 is proposed as evidence of this dispersion. The sidebands on Channel 1 and Channel 4 contain only components with a single phase. Thus, even if dispersion is present, there will be no coherent interference at these channels and thus their powers do not depend on dispersion. The results of Fig. 4 indicate that we can trust Eq. (2) to accurately predict the nonlinear mixing products; however it is evident that dispersion can have a significant impact.

Having characterized nonlinear mixing of a single microwave modulation frequency, we must now characterize the frequency response across the whole band. First, the impact of the AWG filter on the optical spectrum was assessed. Figure 5(a) presents the OSA spectrum of the output at Channel 1 of the AWG in Fig. 3. The AWG is specified with <1 dB ripple, and comparing Fig. 5(a) to Fig. 4, it is evident that the spectrum is unchanged.

#114537 - $15.00 USD Received 20 Jul 2009; revised 8 Oct 2009; accepted 12 Nov 2009; published 1 Dec 2009

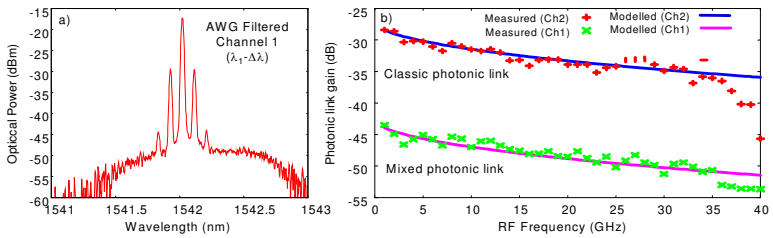

Fig. 5. (a) Optical spectrum of AWG filtered output on Channel 1; (b) Measured photonic link gain of un-mixed: Channel 2 (+) and mixed: Channel 1 (×). Modeled frequency response of a classic photonic link and mixed photonic link including the response of MZM, photo-detector and RF cables and mixing is also presented.

Figure 5(b) presents the link gain obtained when the RF frequency was swept from 1 to 40 GHz and the received RF signal was measured using an ESA.

First, the simple photonic link was characterized by monitoring the signal emerging from Channel 2 of the AWG. Figure 5(b) presents the RF photonic link gain as a function of frequency (note that this is RF link gain which is proportional to the square of optical intensity). The high optical power used on Channel 2 results in a conversion loss of only −27 dB. The link gain response of Channel 2 has the typical form expected for conductor loss, decaying as the square root of frequency. There is no evidence of any degradation due to dispersion supporting the assumption that any dispersion within the HNLF was negligible. The response decays by around 9 dB over the 1-40 GHz band. It should be noted that the total response includes the response of the modulator (3 dB @ 18 GHz), the photo-detector (3 dB @ 40 GHz) and two RF cables (1.5 dB @ 40 GHz). One of the RF cables used degrades significantly at 40 GHz as is evident in Fig. 5(b). A fit incorporating the conductor loss of each of these components is also presented in Fig. 5(b).

The frequency response of the mixing product on Channel 1 was measured by monitoring the AWG output on Channel 1 and again scanning the input frequency. The resulting response is also presented in Fig. 5(b). The form of the response of Channel 1 is identical to Channel 2 but is offset by −16 dB. This is as expected from Eq. (2) and Fig. 4. The carrier mixing efficiency is −19 dB, but recall that the sideband amplitude on Channel 1 is enhanced by 3 dB, resulting in a net signal gain of −16 dB. The fit for Channel 2 has been offset by −16 dB and the match to the response of Channel 1 is excellent. Having characterized the frequency response of the microwave photonic nonlinear mixing, it is now possible to demonstrate the photonic IFM System using optical mixing in HNLF.

5. Photonic IFM using optical mixing in HNLF

Figure 6 presents the system configuration for the photonic IFM. This is similar to Fig. 3; however, both carriers are combined prior to the MZM and are modulated by the same RF signal. The two channels were delayed by different amounts through use of a CFBG which reflects different wavelength channels from different locations along its length. The time delay was 40ps between Channels 2 and 3 and 80ps between Channels 3 and 5. An EDFA amplified both channels to a power of 10dBm before being launched into the HNLF.

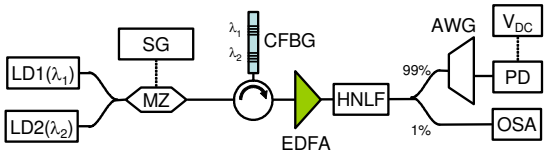

Fig. 6. Experimental setup for the photonic IFM using optical mixing in a HNLF: DFB lasers (LD1 & LD2) provide carriers λ_1 & λ_2 which are combined using a 3 dB coupler. Signal generator (SG) modulates λ_1 & λ_2 via MZ. CFBG delays λ_1 & λ_2. The carriers are amplified and mixed using EDFA and HNLF. Output is monitored using an OSA. AWG isolates $\lambda_1 - \Delta\lambda$ and power is measured using a photo-detector (PD) and analyzed using a voltmeter (V_{DC}).

#114537 - $15.00 USD Received 20 Jul 2009; revised 8 Oct 2009; accepted 12 Nov 2009; published 1 Dec 2009

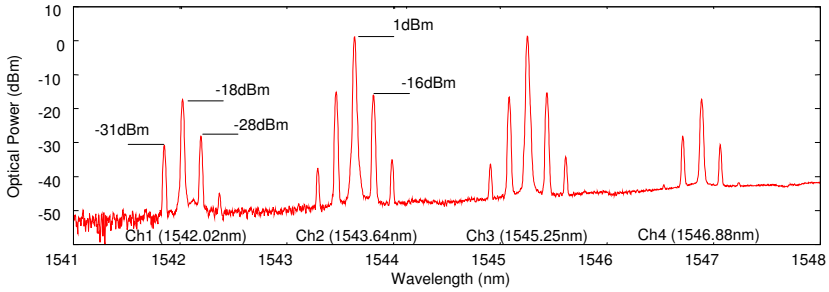

Fig. 7. Optical spectrum at output of the HNLF when mixing Channel 2 and Channel 3, both modulated by a RF tone (22 GHz, 10 dBm). A relative delay of 40 ps is imparted using a CFBG prior to mixing.

To illustrate the behavior predicted by Eq. (5), the system of Fig. 6 was configured with the LD1 and LD2 tuned to Channels 2 and 3 and a 10dBm RF signal at 22 GHz. Figure 7 presents the recorded OSA trace and can be compared to Fig. 4. The original carriers at Channels 2 and 3 are mirror images of each other. The idlers at Channels 1 and 4 are likewise mirror images. The RF sidebands on the idlers are asymmetric indicating that dispersion has resulted in uneven coherent summation of the upper and lower sidebands. This means it is impossible to achieve the maximum and minimum power in both side-bands simultaneously which will impact the IFM system response, particularly at high frequencies.

To demonstrate the photonic IFM, the system of Fig. 6, was configure with LD1 and LD2 tuned to Channel 2 and Channel 3 respectively. The RF signal was swept from 1 to 40 GHz with a power of 0 dBm. The optical power at Channel 1 of the AWG was recorded as a function of frequency using a DC voltmeter. Figure 8(a) presents the measured IFM frequency response. Oscillatory behavior is clearly evident with a period of approximately 25 GHz as expected due to the 40 ps time delay introduced by the CFBG. A reduction in oscillation amplitude with increasing frequency is observed. It is anticipated that this will have a modest impact on system sensitivity at higher frequencies. This amplitude reduction can be attributed to frequency response of the optical modulator (as demonstrated in Fig. 5(b)) which had a nominal bandwidth of 10GHz, but degrades gracefully to 40GHz. An improved response could be achieved if a modulator with a 3dB bandwidth of 40GHz were employed.

The frequency response of the system has been modeled using the data from Fig. 4, Fig. 5 along with Eq. (5). The modeled frequency response of Fig. 5(b) has been used with the response of the photo-detector and the output cable removed (since these are now operating at DC). The chromatic dispersion introduced by the gratings has been modeled as linear with frequency, and thus the phase may be described as $\phi_i = D_i\omega^2$. The dispersion in Eq. (5) was manually adjusted to provide the best fit to the measured data. This fit was achieve with,

$$(\varphi_1 + \varphi_4) = 1.27\times10^{-5}\,\omega^2, (\varphi_2 + \varphi_3) = -2.53\times10^{-5}\,\omega^2 \qquad (6)$$

With the exception of the dispersion, no other fitting or scaling parameters were used in obtaining the modeled response. The fit between the modeled and measured response is excellent. It should also be noted that the stability of the system output was also excellent.

To demonstrate the flexibility of this IFM system of Fig. 6, the optical wavelength channels LD1 and LD2 were tuned to Channel 3 and Channel 5 (1548.51 nm) to increase the relative delay between the channels to 80 ps. Despite the greater wavelength separation, between Channel 3 and Channel 5, the mixing gain of the HNLF is almost identical to that of Channel 2 and Channel 3. The optical power was again set to 10 dBm and the power output on AWG Channel 1 was again recorded as a function of the frequency of the input RF signal.

#114537 - $15.00 USD Received 20 Jul 2009; revised 8 Oct 2009; accepted 12 Nov 2009; published 1 Dec 2009

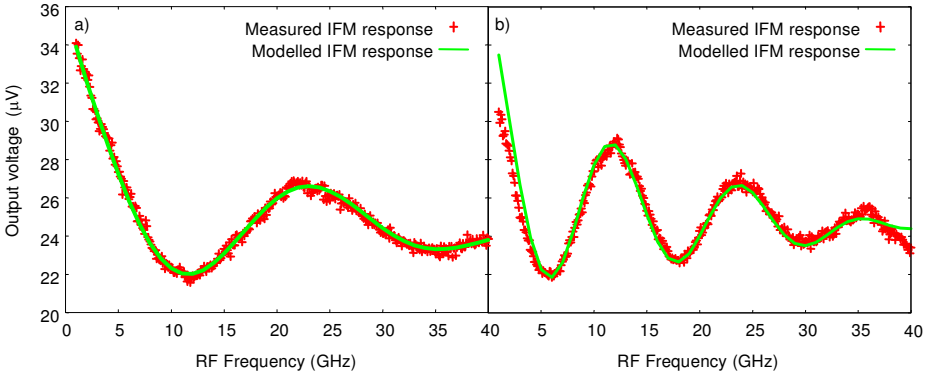

Fig. 8. IFM frequency response a) mixing Channel 2 and Channel 3 ($\Delta\tau$ = 40ps); b) mixing Channel 3 and Channel 5 ($\Delta\tau$ = 80ps). The modeled response of Eq. (5) including the dispersion of Eq. (6) and Eq (7) respectively are also shown.

Figure 8(b) presents the frequency response of the IFM formed by mixing Channel 3 and Channel 5. Comparing to the response of Fig. 8(a), the oscillation period is approximately 12.5 GHz as expected with the delay of 80 ps. The model of Eq. (5) was adjusted by doubling the time delay, and fine tuning only the dispersion parameters to

$$(\phi_1 + \phi_4) = 1.27\times10^{-5}\omega^2, (\phi_2 + \phi_3) = -3.8\times10^{-5}\omega^2 \quad (7)$$

The match between the predicted and measured responses in Fig. 8(b) is also excellent.

Since we have an accurate and reliable model of the IFM output response, we can now use this response to interpret the IFM output as a frequency measurement. Provided the RF signal power is known, the frequency response of Eq. (5) is fully defined for a given selection of two wavelength channels. To measure frequency of the RF signal, Eq. (5) was inverted and used to map measured power to interpreted frequency. Since Eq. (5) is not one-to-one, a band of operation must be assumed in order to make an unambiguous measurement.

Figure 9(a) and Fig. 9(b) present the interpreted frequency obtained by inverting Eq. (5) and inserting the measured data from Fig. 8(a) and Fig. 8(b), respectively. Figure 9(a) has four distinct bands where output power maps to only one input frequency. Figure 9(b) has six such bands. The interpreted frequencies are very close to the ideal values across each band, an error of 5% is achieved for most frequencies, with larger errors observed at the edges of each band as expected. The photonic IFM using mixing in HNLF was thus been successfully demonstrated.

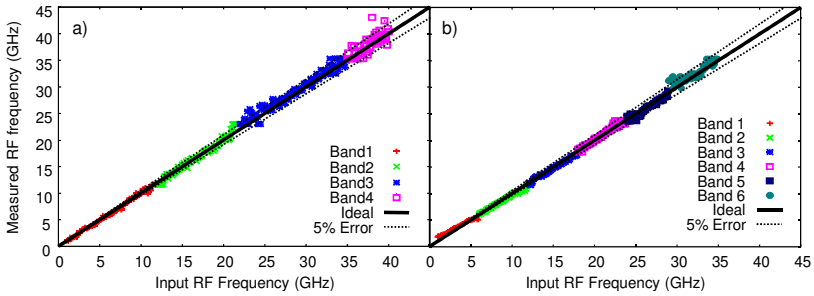

Fig. 9. Frequency measurement a) mixing Ch 2 and Ch 3; and b) mixing Ch 3 and Ch 5.

#114537 - $15.00 USD Received 20 Jul 2009; revised 8 Oct 2009; accepted 12 Nov 2009; published 1 Dec 2009

6. Discussion and conclusions

We have proposed a novel IFM system that exploits FWM in HNLF and have derived a simple, first principles model of the system response, accounting for dispersion, microwave photonic bandwidth and mixing efficiency. An implementation which is responsive from 1 to 40 GHz has been demonstrated. The key feature of this implementation is that no high speed electronics was required at any stage of the system which is a major advancement over previously reported microwave photonic implementations [8]. Agreement between the measured results and predictions was excellent. The system stability was also excellent.

The system sensitivity and dynamic range must be fully analyzed and optimized. We are currently exploring more accurate models of the system dispersion, elimination of the ASE on the output channels prior to mixing and the use of lock-in techniques [19].

The system demonstration of Figs. 9(a) and 9(b) exhibited a number of distinct bands. It would be possible to configure the system with a shorter relative delay (12ps) and achieve an unambiguous, monotonic response from 1 to 40GHz, however this would come at the expense of reduced sensitivity. To retain the sensitivity achieved in Fig. 9(b), while also operating over the 1-40GHz band, it would be necessary to implement several IFMs in parallel [17,20]. Using a binary discrimination scheme, 3 parallel IFMs could distinguish between 8 bands. We are currently exploring techniques to implement multiple parallel IFMs. It should be noted that since the HNLF, EDFA, AWG, CFBG and MZM can each operate on multiple parallel wavelength channels simultaneously, each new IFM should require only the addition of one laser source and one detector to the system minimizing additional cost and complexity.

The demonstrated responsiveness of this photonic system up to 40GHz and the demonstrated ability to reconfigure the system by simply adjusting the wavelength channels offers clear advantages over existing electronic implementations [17]. However, the true potential of this approach will only be realized once multiple parallel IFMs can be implemented using a single set of photonic hardware. The implementation of multiple parallel IFMs using this HNLF system is currently under investigation.

Acknowledgments

The support of the Australian Research Council through its Centers of Excellence program is gratefully acknowledged.

#114537 - $15.00 USD Received 20 Jul 2009; revised 8 Oct 2009; accepted 12 Nov 2009; published 1 Dec 2009